

Monte Carlo Simulations of DNA Damage and Cellular Response to Hadron Irradiation

M. Loan^{a,b*}, B. Freeman^c, A. Bhat^d, M. Tantary^e, M. Brown^d and K. Virk^c
(KCST-CVMC Collaboration)

^aDepartment of Physics, Kuwait College of Science and Technology, 28007, Kuwait

^bANUC, Australian National University, Canberra, 2000, Australia

^cDepartment of Computer Science, Kuwait College of Science and Technology, 28007, Kuwait

^dDepartment of Oncology, Clinch Valley Medical Center, Richlands, Virginia, 24641, USA

^eDepartment of Internal Medicine, Clinch Valley Medical Center, Richlands, Virginia, 24641, USA

^cDepartment of Computer Science, Kuwait College of Science and Technology, 28007, Kuwait

(Dated: November 20, 2019)

Numerical simulations are performed on a stochastic model based on Monte Carlo damage simulation process and Markov Chain Monte Carlo techniques to investigate the formation and evaluation of isolated and multiple DNA damage and cellular survival by light ionizing radiation in a colony of tumour cells. The contribution of the local clustering of the strand breaks and base damage is taken into account while considering double-strand breaks (DSBs) as primary lesions in the DNA of the cell nucleus induced by ionizing radiation. The model incorporates the combined effects of biological processes such as the tumour oxygenation, cellular multiplication and mutation through various probability distributions in a full Monte Carlo simulation of fractionated hadrontherapy. Our results indicate that the linear and quadratic parameters of the model show a negative correlation, for protons and helium ions, which might suggest an underlying biological mechanism. Despite using a model with quite different descriptions of linear and quadratic parameters, the observed results for linear parameter show largely reasonable agreement while the quadratic parameter consistent deviations from the results obtained using the LEM model at low LET. In addition to the LET dependence, RBE values showed a strong dependence on α/β ratio and a considerable scatter for various particle types indicate particle specific behaviour of initial its slope. The surviving curves show a non-linear dose-response suggesting that interaction among DSBs induced by ionizing radiation contribute significantly to the quadratic term of the model. Nonetheless, our simulation results suggest that not only is the model suited for effectively predicting the relative biological effectiveness of the charged particles at low LET and different survival, but also to accuracy in prediction of cell-killing in radiotherapy such as hadrontherapy.

Keywords: Monte Carlo simulations, DNA damage, RBE, cellular response, hadrontherapy

I. INTRODUCTION

Hadron radiotherapy, one of the established modalities for the treatment of cancer-based on irradiating tumours with accelerated light ions is a promising method for the treatment of specific types of cancer [1–8]. Their dose-distribution characteristic culminating with higher rate of energy loss at the end of their ranges, resulting in a sharp decrease beyond the Bragg peak allows for a high conformity to the deep-seated tumours while sparing healthy tissues [9–12]. With the range modulating techniques to spread out the Bragg peak to cover the whole target, the ionized dose is delivered with a spectrum of different linear energy transfers (LET) at each point in the spread-out Bragg peak. Since the high-LET component has an increased biological efficiency resulting in the induction of enhanced and unreparable biological damage, quantified in terms of Relative Biological Effectiveness (RBE), the ionized particles show enhanced biological effectiveness in eradicating the tumour cells [13–17]. Apart from protons, the most frequently used ion species is carbon; however, heavier ions such as oxygen are available in some centers too, and irradiation with lighter ions such as helium or lithium may be advantageous for some tumours.

The induction of radiation-induced DNA breaks is of central importance of radiation-induced cell death. The reproduction of the radiation-induced yield of single- and double-strand breaks is taken as a benchmark for numerical simulation models for the estimation of the radiation damage to DNA. Differences in the biological response induced by ionized particles protons compared to photons reported in last few years raise the concerns regarding the analysis of DNA damage induction and processing. Besides producing approximately 20-25 times more single-strand breaks (SSBs) than double-strand breaks (DSBs) per grey and a base damage of 2,500-25,000 per grey per cell in a typical mammalian cell [18–20], low-LET ionized radiations effectively produce multiple damage sites (MDS) consisting of

* Corresponding author

two more strand breaks or base damage within a few turns of DNA helix. These strand breaks are detected as an SSB in most experimental studies. Whereas, DSBs and MDS act as the primary cause of cell kill by the radiation.

DNA isolated and multiple strand break inductions by different radiation qualities show that clear differences emerge when looking at the rejoining process [21–24]. The lack of a general relationship between cellular effects with respect to radiation quality has made the precise measurements of DSBs and MDS with radiation quality. Earlier measurements of yields of strand breaks showed approximately slight or no variation with radiation quality. Some earlier studies reported the relative biological effectiveness (RBE) for induction of DSBs by the protons relative to 200–250 keV/ μm x-rays radiations vary between 0.8 and 1.1 using the sedimentation technique as well as filter elution [25–28]. Data on RBE for induction of DSBs in human cells using protons, helium and carbon ions up to about 120 keV/ μm were reported in the range 1.35 which is much lower compared to that for cell killing and malignant cell transformation [21, 29–31]. These data are in contrast to RBE values of 2.6 for induction of DSBs found in yeast using 120 keV/ μm helium ions using neutral sedimentation. These significant differences in RBEs for induction of SSBs and DSBs, as well as the cellular effects, reflect different reparability of strand breaks as a function of radiation quality.

The ideal use of hadron therapy heavily relies on modelling [32–35]. Clear understanding of physical and biological processes underlying the hadro-biological the mechanism is essential for the optimal uses of treatment planning. However, existing hadrontherapy treatment planning approaches are largely based on the effectiveness of the physical processes involved compared to the the biological response elicited in cells and tissues by hadrons and ions. Most of the treatment planning is based on interpolating the linear-quadratic (LQ) parameters of LQ fits the experimental data on surviving curves while assuming similarity in biological effects among heavy ions species of similar LET values [36–38]. This indicates that the biological processes of damage induction and repair have not been considered explicitly and is reflected in the large uncertainties that can be found in the literature regarding the α , β parameters of the LQ model and in the definition of RBE-LET relationship for light and heavy ions. More generally, evidence has also been reported showing *in vitro* measurement with V79 cells having a low α/β while *in vivo* experiments showed a high α/β ratio [13]. Since RBE has a dependence on this ratio, a direct quantitative comparison between these measurements will be misleading. The published data on RBE values also showed large fluctuations in RBE data in tumour cells, as well as in neighbouring healthy tissues [39].

An alternative approach is to incorporate the biological parameters into the ionized radiation response models. This has gained considerable attention including numerous analytic and numerical models which seek to include physical as well as biological effects. A very significant improvement on the front has been achieved in some most recent studies on track structures and resulting DNA damage and repair processes through pathways, suggesting a non-trivial relationship between radiation-induced DSBs in the cell nucleus and their LET dependencies as well as the on the probability of cell death induced by the DSB effects [40–44].

The aim of this study is to build on and extend the previous detailed description of recently published hadrontherapy models on radiation-induced DNA strand breaks, DNA repair, and cellular survival [40, 43]. Whereas the mixed beam models, such as the micro-dosimetric kinetic model (MKM) [45, 46], the local effect model (LEM) [47–49], and the mechanistic models including repair-misrepair fixation (RMF) model [50] and BIANCA model have been successful in allowing to predict the relationship between physical parameters of radiation and cell survival, we use the mechanistic model proposed by Wang *et al.*, [40] in this study as this model offers predictions at the molecular and cellular levels that are quantitatively described by only two input parameters; the average number of primary particles that cause DSB, and the average number of DSBs yielded by each primary particle that caused DSB. Furthermore, the model provides a simpler structure in terms of the quantification of the effects of dependence of linear and quadratic components on LET and dose and calculation of RBE for the same type of cells exposed to different particle species at different LET.

Considering that DSBs are the initial lesion in the DNA of the cell nucleus induced by ionizing radiation, compared to DSBs that occur spontaneously during cellular processes at quite significant frequencies, while taking into account the non-homologous end-joining pathway as domain pathway of DSB repair in mammalian cells, we simulate a modified model that incorporates biological processes such as adaptive response and hypoxic effects with sufficient number of randomly selected cells surpassing the approximate avascular growth phase and approaching clinical levels. The induction of radio-adaptive response in the model signifies the ability of low dose radiation to induce cellular changes that alter the level of subsequent radiation-induced or spontaneous damage. These effects appear to be especially crucial in the case of exposure to low doses and dose rates of ionizing radiation [51–58]. Recent studies have shown that there is conclusive evidence for some cells that radio-protection induction from an adaptive response may be activated by a few or single charged particle track traversals through the sensitive region of individual cells [59–63]. Equally important is the incorporation of radiobiological differences between acute and chronic hypoxic cells. The modified model simulates chronically hypoxic cells that may have low or depleted energy reserves which would impair their repair mechanisms in contrast with acutely hypoxic cells that are repair competent. Hypoxia is modelled through the oxygen level allocation based on pO_2 probability distribution.

The improved model also attempts to address the discrepancies and fluctuations in RBE observed in the results of

different experiments and the lack of complete inclusion of the underlying biological processes with light ions, especially in the low LET region, by attributing the roles played by biological parameters such as tissue type, oxygenation level, and balance between an increase in radiation induced DSB yield and increased loss of DNA fragments induced along the track of primary particles. Monte Carlo simulation in this LET region will be highly useful until a more detailed knowledge of these effects is available.

The rest of the paper is organised as follows: A probabilistic model, that incorporates the combined effects radiation-induced isolated and multiple DNA strand breaking, adaptive response, tumour oxygenation, cellular multiplication, and mutation in a full Monte Carlo simulation of fractionated hydrotherapy is outlined in Sec. II. The details of hybrid Monte Carlo techniques to simulate a random cell number, sufficient enough to surpass the approximate avascular exponential growth phase to reach a cell colony at the clinical level, within a nonspatial environment, is given in Sec. III. We present and discuss our results in Sec. IV. Here, the improved probabilistic model results, with stochastic biophysical input, are validated and compared with results obtained by various other simulation and experimental studies. In particular, a systematic comparison of linear and quadratic parameter predictions of the improved model with those of LEM model is of interest, since LEM model is already used by treatment planning systems of European dual ion therapy facilities for biological optimization in carbon ion therapy. Section V is devoted to the summary and concluding remarks. We hope that the quantitative approach illustrated here will facilitate improvements to our understanding of physical and biological processes, in hadrontherapy, that will no doubt become possible and necessary as additional experimental evidence becomes available.

II. IMPROVED PROBABILISTIC MODEL WITH STOCHASTIC INPUT

A. Cell Survival Model

The probability distribution of cell death with radiation in a fully oxic population can be described in LQ theory by an equivalent equation:

$$P_{ox}(D) = 1 - \exp(-\alpha D - \beta D^2)$$

where the linear component α characterizes a single lethal event made by one-track action and the quadratic component α_2 characterizes the accumulation of sub-lethal events made by two-track action for oxic conditions. However, both these events describe the DNA double-strand breaks and do not take into account the damage caused by the DNA single-strand breaks. Studies have shown that single-strand damage caused by x-rays is far more than the number of double-strand damage [64–66]. Also, both the experimental and model studies on isolated and multiple strand damage by the ionizing radiation and repair process [40–44, 67, 68], have shown that the conventional linear-quadratic model is poorly suited to understanding these factors, as its empirical parameters are only indirectly linked to the mechanistic drivers of radiation response, making it difficult to predict quantitatively the impact of a given mutation. This is particularly true when multiple genes are mutated, as occurs commonly in cancer.

To simulate the cell death probability due to charged particle irradiation, we use the recently proposed mechanistic model that incorporates the kinetics of cell death induced by the DSBs effect and DNA repair through different pathways and cell death processes [40]. The model describes the yield of radiation induced DSBs through contributions of interaction among DSBs induced by different primary particles described by the average number of primary particles which caused DSB and DSBs induced by single primary particle and their interactions, including the cluster DNA damage effect and the overkill effect by the average number of DSBs yielded by each primary particle that caused DSB.

Assuming that the number of DSBs yielded by the primary particle is Poisson-distributed ¹, the average number of primary particles that cause DSBs is given by

$$n_p = \frac{YD}{\lambda}(1 - e^{-\lambda})$$

and the average number of DSBs yielded by each primary particle that caused DSB is given by

$$\lambda_p = \frac{\lambda}{1 - e^{-\lambda}},$$

¹ For light and heavy ions at high LETs, the deviations of lethal lesions from Poisson distribution are significant. It is argued that increasing LET causes deviation from the Poisson distribution by non-random clustering of lethal lesions in some cells

where $\lambda = (N/n)$ is the DSB yield per cell per primary particle that depends on average number of radiation-induced DSBs per cell, $N (=Y \times D)$ and number of primary particles, n ($\propto 1/LET$) passing through the nucleus.

The model considers the repair of DSBs through nonhomologous end-joining (NHEJ) pathway as the dominating pathway in mammalian cells and assigns the probability of a DSB being correctly repaired as

$$P_{correct} = \mu_x P_{int} P_{track},$$

where

$$P_{int} = \frac{1 - e^{\eta(\lambda_p)n_p}}{\eta(\lambda_p)n_p} P_{track} = \frac{1 - e^{\xi\lambda_p}}{\xi\lambda_p}$$

μ_x is the average probability of DSB end joining with the other end from the same DSB correctly with μ_y as the sensitivity of an error repair and where $\xi\lambda_p$ is the average probability of a DSB end being joined with a DSB end from a different DSB induced by the same primary particle. Finally, the probability of a DSB contributing to cell death is given by

$$P_{contrib} = \frac{1 - e^{\phi\lambda_p}}{\phi\lambda_p}$$

The average number of lethal events, N_{death} , is then given by

$$N_{death} = \mu_y \times P_{contrib} \times (1 - P_{correct})$$

This results in the following probability model, with the similar form as the LQ model, for the cell death [40]:

$$P_{ox}(D) \propto \left[1 - e^{-\alpha D - \beta D^2}\right], \quad (1)$$

where

$$\alpha = Y \times \left[\frac{1 - e^{\phi\lambda_p}}{\phi\lambda_p} \right] \times \left[1 - \mu_x \left\{ \frac{1 - e^{\xi\lambda_p}}{\xi\lambda_p} \right\} \right] \times \mu_y \quad (2)$$

$$\beta = \frac{1}{2} \eta(\lambda_p) \frac{Y}{\lambda_p} \times Y \times \left[\frac{1 - e^{\phi\lambda_p}}{\phi\lambda_p} \right] \times \left[1 - \mu_x \left\{ \frac{1 - e^{\xi\lambda_p}}{\xi\lambda_p} \right\} \right] \mu_x \mu_y. \quad (3)$$

are the improved model linear and quadratic parameters, respectively. The functional dependance of α and β on the LET and dose D can be seen through λ , n_p and λ_p . Since at low-LET, dose response of DSB induced by radiation is linear, therefore the cell survival curve is in agreement with the LQ model. However, for high-LET radiations, when delivering the same dose to the nucleus as low-LET radiations, the number of primary particles causing DSB is much smaller, and the contribution of interaction among DSBs induced by different primary particles to cell death would be vanishingly small, therefore the cell survival curves tend to follow the the exponential models [40]. The dependence of alpha and beta on the dose range has shown an impact on the alpha/beta ratio determined from the survival data [69, 70]. The low-dose region had a significant influence that could be a result of a strong linear, rather than quadratic component, hypersensitivity, and adaptive responses. Such a dependence serves as a caution against using cell survival data for the determination of α/β ratio.

The model is further improved by quantifying the biological effect of oxygen concentrations on tumour cells in terms of the oxygen enhancement ratio (OER). Assuming that (i) the damage response of DNA single-stranded breaks and double-stranded breaks are two relatively independent processes involving different signaling pathways, (ii) oxygen distribution in tissue has a cylindrical symmetry, and (iii) each hypoxic cell as well as each capillary consumes oxygen spatially at an equal and constant rate (no intravascular resistance), the improved cell death probability can be modelled by the joint probability distribution

$$p_{hyp}(D) \propto \left[1 - e^{-\alpha_m D \cdot OER(D,L,p) - \beta_m D^2 \cdot OER^2(D,L,p)}\right] \quad (4)$$

The OER is determined from dose-LET and pO_2 dependent model [71]

$$OER(D_h, L, p) = \frac{2D\alpha_2(L, p)}{\Phi(L, p) - \alpha_1(L, P)}, \quad (5)$$

where

$$\Phi(L, p) = \sqrt{\rho_1^2(L, p) + 4\rho_2(L, p)(\rho_1(L, p)D_h + \rho_2^2(L, p)D_h^2)}.$$

The dependence of ρ_i on pO_2 and LET, in the clinically relevant LET region, is given by

$$\begin{aligned}\rho_1(L, p) &= \frac{(a_1 + a_2 \cdot L) \cdot p + (a_3 + a_4 \cdot L) \cdot K}{p + K} \\ \rho_2(L, p) &= \rho_2(p) = \frac{(b_1 \cdot L) \cdot p + b_2 \cdot K}{p + K},\end{aligned}$$

where L is linear energy transfer, a_i and b_i are constant coefficients [72] and K represents the oxygen concentration around 2.5 – 3 mmHg. Eq. 5 can be used to describe the *OER* for various different radiation types at low- and high-LET regions and for various oxygen levels relevant to theoretical and clinical situations. We observe the model predictions relative to the oxygen effect with light and heavy ion irradiation and compare the results with preclinical and clinical studies.

Equation (4) is randomly simulated to determine the probability of cell death from its surviving probability. We will examine and compare the effects on the slopes of the survival curves for both well-oxygenated and hypoxic tumours for low- and intermediate LET hadrons and charged ions using a hadron specific approach. Since the *OER* for protons is similar to x-rays [73–75], namely 2.5 to 3, it will be interesting to know how will the different fractionation schedule affect *OER*. This is particularly important in light of the ambiguous relationship between tumour oxygenation and the model parameters, α and β .

B. α/β ratio and RBE characterization

The ratio of intrinsic parameters, α and β , of the LQ model, is a measure of the fractionation sensitivity of the cells. The cells with a lower α/β are more sensitive to the sparing effect of fractionation. The determination of hadrotherapeutic outcome and therapeutic window strongly depends on a reliable estimation of parameters α , β and α/β . Because of the mechanistic nature of the above model, it can be directly extended to validate the DSB distribution caused by x-rays and charged particles. Therefore, the model is able to make predictions for α/β ratio and RBE at a different survival with hadrons and heavy charged ions. The modelled parameters α and β for the same type of cells irradiated by different radiation types at different LET can be used to reflect on the ratio α/β as an indicator of cellular repair capacity. Using Eqs. (2) and (3), the ratio α/β is given by [40]

$$\alpha/\beta = \frac{1 - \mu_x \left(\frac{1 - e^{-\xi \lambda_p}}{\xi \lambda_p} \right)}{(1/2)\mu_x \eta(\lambda_p) Y / \lambda_p}, \quad (6)$$

where η for a given track is determined by the distribution of DSBs created by the track. The ratio is dominated by the interaction of DSBs induced by different primary particles in the limit $\lambda_p \rightarrow 1$ for photons and low-LET irradiation, whereas for hadrons and ions at higher LET, the ratio is attributed to Y/λ_p . Because RBE values involve two parameters of LQ model, we input the role of improved α/β ratio to obtain the explicit dependance of RBE on the hadron dose as well as the LET from selected hadron:

$$RBE(L, D, (\alpha/\beta)_x) = \frac{1}{D_p} \left[\sqrt{\frac{1}{4} \left(\frac{\alpha}{\beta} \right)_x^2 + \Gamma} - \frac{1}{2} \left(\frac{\alpha}{\beta} \right)_x \right], \quad (7)$$

where

$$\Gamma = \left(\frac{\alpha}{\beta} \right)_x \frac{\alpha(L)}{\alpha_x} D + \frac{\beta(L)}{\beta_x} D^2.$$

We compare the our Monte Carlo estimates for cell-survival fraction to the experimental data to validate the accuracy of the above RBE model.

III. MONTE CARLO IMPLEMENTATION

A. Hybrid Algorithm

The numerical simulations were divided into two parts; the first part of the hybrid algorithm uses Monte Carlo damage simulation (MCDS) algorithm [76] to simulate the formation of isolated and multiple damaged DNA sites by radiation of various species and different LETs. This algorithm captures the trend in DNA damage spectrum with the possibility that the small-scale spatial distribution of elementary damages is governed by stochastic events and processes [77]. The use of this quasi-phenomenological algorithm is to provide nucleotide-level maps of the clustered DNA lesions, including simple and complex forms of the single-strand break (SSB) and DSB and to avoid the initial simulation of the chemical processes. This algorithm also allowed a range of particle energies has been expanded, and the induction of damage for arbitrary mixtures of charged particles with the same or different kinetic energies can be directly simulated. To examine the effects on damage complexity of the direct and indirect mechanisms, a modified version of MCDS algorithm was used to mimic reductions in the number of strand breaks and base damages associated with exposure to an extrinsic free radical scavenger, dimethyl sulfoxide, that offers protection against both strand breakage and base damage.

The second part uses a stochastic Monte Carlo technique to simulate the evaluation of cell survival. Accordingly, the hybrid code is divided into two different parts of which each uses different Monte Carlo algorithms. Radiation-induced DSB yield per cell per Gy and DSB yield per cell per primary particle were directly obtained with MCDS algorithm. These parameters were used to estimate the initial slopes of linear and quadratic coefficients for the later use in the stochastic Monte Carlo algorithm for the evaluation of cell survival. The software evolved from the MCDS code and many routines were adapted from an existing stochastic serial code to return a large-scale framework despite the different target theory. Each part of the hybrid code is configured to output its own intermediate results so that code can be validated against the results from various numerical and experimental methods.

The stochastic Monte Carlo technique [78, 79] is used to develop the dynamics of cell death governed by Eq. (4) using a predefined fractionation schedule of one irradiation per day. The Monte Carlo algorithm employed consists of a nested numerical loop over radiation dose, a loop over the time steps, a loop over oxygen supply, a loop over the age of each initial cell and a loop over the cells. At each step, the cells may exhibit the possible altered states or division. The algorithm uses continuous and differentiable probability distribution relationships to describe the biophysical effects of cell colony. At each time step, a stochastic tree of probabilities is applied to every i -th cell which alters the state of the cell depending on whether it has been irradiated or not. The modification in the probability tree can be made easily and new branches can be added to incorporate additional biological effects or modify ones detailing the mechanism in cell eradication.

A regular grid of capillary cells is used to initiate the oxygenation. To ensure a significant supply of oxygen for the tumour cells, a regular grid of capillary cells is used. As the tumour cell splits, the daughter cells are placed at the adjacent positions extended in the direction of the tumour boundary. For an occupied position, the respective cell is shifted to one of its neighbouring positions. The shifts are repeated iteratively until a free grid position is available. Our simulation results focus on simulating oxic, moderately hypoxic and severely hypoxic tumours while assigning uniform, log-normal and normal probability distributions of pO_2 values based on published data [80, 81] to allocate cellular oxygenation. Compared to earlier models that simulate spatial oxygenation distributions by assuming a spherical geometry and use the radial distances of cells from the tumour periphery to determine oxygenation [82–84], this technique method of allocating oxygenation levels from a pO_2 probability distribution is simple and user-friendly and has the advantages of flexibility as it easily allows for the pO_2 distributions and variation during the growth or treatment in a single simulation, if required. It also enables easy expansion of the model to more refined forms relationships between the oxygen allocation and probability distributions during future studies [80].

We start the algorithm with a colony of 10^6 cancer cells with the age of each initial cell in the interval [1, 50] drawn randomly from a uniform distribution. Taking into account the volume of a single cell and the volume of related intercellular space, this corresponds to a class I spherical volume of approximately 500mm^3 . The cell division algorithm was designed with high computational efficiency. To optimize the algorithm and make modifications to allow for more memory efficient data storage, the colony is arranged as an array for an efficient way to store, access and manipulate data as the tumour cells die, split, mutate and accumulate in the ensemble. However, the method does not allow us to work with geospatial clustering effects due to its lack of dimensionality but allows for rapid computation.

The hadrontherapy begins with a virtual tumour colony with a pre-defined death probability and hypoxic status. Cells continue to divide between the fractions during the simulated hadrontherapy and fractionated treatment continues until all tumour cells have been eradicated or the desired number of treatment fractions has been delivered. Cell death is accessed for each cell in the array for each dose fraction. After cell death, links in the array are updated to maintain the consecutive order of the cells in the relevant hourly list as well as the number of living cells. The emptied

array elements are auto-reused after cell death for efficient computer memory usage. We observed a computation time of 2-3 minutes/trajectory to run an ensemble of 10^6 cells with fractionated hadrontherapy, with the exception of rapidly repopulating tumours.

B. Input Parameters and Simulation Details

The hybrid algorithm contains a number of input parameters which intuitively describe physical and biological effects of the interaction of light ions with tumour cells. These parameters include natural death rates, natural cell repair probabilities, cell division and multiplication probabilities, spontaneous mutation rates, etc. The exact values of these parameters can be taken from experimental results, if identified, otherwise the parameters are simulated. However, the experimental determination of some of these parameters is rather challenging and in many cases, it involves the assumption of a model relating a measured quantity to the quantity to be determined. The input parameters were applied in the model after analyzing for physical observables over a reasonable range of estimated values or probability distributions. Since the key input parameter values often vary during treatment simulations, a graphical user interface (GUI) was developed within the Python environment to enable convenient values of the desired input parameters. This also allows the running of multiple batches run iterating over different random seed numbers and ranges of input parameter values.

To generate a random integer sequence, a set of random floating point number between 0 and 1 with a uniform, normal, lognormal or exponential distribution, we utilized the Ziggurat pseudo random number generator [85]. The object-oriented programming language Python was used to create the model algorithm. The numerical loops contain the trees of probabilities drawn from several probability distributions describing various biological effects. Following [79] we calculate, for time step Δt , the probability that each cancer cell (i) is irradiated by a hadron or ion; (ii) is killed by a single precise hit of the radiation; (iii) naturally dies; (iv) naturally multiplies - the daughter cell is also cancerous; (v) dies due to cell's radiosensitivity; or (vii) remains unchanged. In case the cancer cell is not irradiated, it can die naturally, multiply or stay intact. For each Monte Carlo run, the tumour cell system evolves in time according to the probabilities defined above. The Pseudo random numbers are generated to sample probability distributions based on model calculations describing the above events.

The trees of probabilities of the above seven scenarios form input data and are presenting in Tab. I. Some of the probabilities, e.g., the probability of natural death of a cancer cell, probabilities of the division of cancer and mutated cells, can be approximated by constant values extracted from the experimental data or simulation results. Remaining probabilities in the above net describing the biological and physical effects of the interaction of ionizing radiation with cancer cells are drawn from probability distributions. For example, The distribution of hits is given by the binomial distribution, which for a large number of cells may be approximated by the Poisson distribution.

The probability of hitting a cancer cell by radiation can be drawn from the binomial distribution, which for a large number of cells may be approximated by the Poisson distribution, as well as from a stretched exponential distribution. However, we draw the probability, P_{hit} , form a quasi-linear probability distribution, $P(D) = 1 - e^{-c_1 \cdot D}$, where D is the dose per single cell per time step and c_1 is a scaling constant. Such distribution can also be used for the death of irradiated cancer cells because of its specific radiosensitivity, P_{CRD} . On, the other hand, the probability distribution for cancer transformation, P_{RC} , is well described by sigmoidal probability distribution [86] with critical index n , $P(Q) = 1 - e^{-aQ^n}$, where Q is the number of mutations and constant a . This distribution, however, does not take into account the cancer-cell microorganism mutations that arise non-homogeneously over time.

The tumour was exposed to hadron and ion radiation dose of 2 - 5 Gy per day up to a maximum dose of 10 Gy. By varying the random seed number in the hadrontherapy algorithm, we generate six ensembles of cell irradiation measurements for each dose value for later analysis. The expectation values and statistical error estimates of the observables from Monte Carlo simulations were estimated using the jackknife method. The statistical errors were estimated by grouping the stored measurements into 5 blocks, and then the mean and standard deviation of the final quantities were estimated by averaging over the "block averages", treated as independent measurements. The estimate of the error of observable ρ was calculating by using

$$\delta\rho = \sqrt{\frac{M-1}{M} \sum_{m=1}^M (\bar{\rho}_m - \langle\rho\rangle)^2}.$$

Statistical significance between two data sets was accessed using a 2-tail t -test with a 95% confidence interval.

!ht

TABLE I: Input parameter values tumour growth, radiation-induced DSBs for V79 and probabilities used for the simulations.

Parameters (Ref)	Value
<i>Tumour growth</i>	
Number of cancer cells	10^6
Cell diameter	$20 \mu\text{m}$ [87]
Radius of capillary cells	$10 \mu\text{m}$ [87]
P_{O_2} threshold for hypoxia	5 mmHg [87]
Maximum OER (p)	3 [88]
Maximum K at OER	3 [88]
<i>Radiation-induced DSBs for V79 cell</i> [40]	
μ_x	0.956(23)
μ_y	0.030(17)
ζ	0.041(20)
ξ	0.060(38)
$\eta\lambda_p \rightarrow 1$	$9.78(10) \times 10^{-4}$
$\eta\lambda_p \rightarrow \infty$	0.0065(1)
<i>Probability distributions</i> [78, 79]	
Spontaneous mutation in a cell	$(1 - \tau)(1 - e^{-aK^n}) + \tau$
Natural repair of one mutation	δe^{-aK^n}
Mutation develops in the irradiated cell	$1 - e^{-const \cdot D}$
Mutated cell \rightarrow cancer cell	$1 - e^{-const \cdot D}$

IV. RESULTS AND DISCUSSION

A. Yield of radiation-induced DSB and α/β ratio

The DNA damage induced by ionizing radiation was obtained in terms of isolated and multiple strand breaks. Fig. 1 shows the dependence of the yield of radiation-induced DSB ($\text{Gy}^{-1}\text{cell}^{-1}$) of V79 cells on LET. We notice that at low and medium LET, DSB yields generally increase with increasing LET, from ~ 45 per Gy per cell at $1.2 \text{ keV}/\mu\text{m}$, up to $98 - 102$ per Gy per cell at $300 - 550 \text{ keV}/\mu\text{m}$. The calculated yield of DSBs after irradiation with protons showed an interesting feature with LET around $15 \text{ keV}/\mu\text{m}$. At LET below $12 \text{ keV}/\mu\text{m}$, the DSB yield per track, λ increases sharply with LET, however, λ_p , the average number of DSBs yielded by each primary particle that causes DSB increases rather slowly and is nearly similar to that with γ . This may explain the reason behind nearly similar biological effectiveness of low LET protons and photons. For proton LET above 12 the total yield showed a decrease of about 15% with increasing LET within the range $13 - 52 \text{ keV}/\mu\text{m}$. Such effects were also observed in other studies with varying percentages of yield reduction [89, 90].

At high LET values, the total yield of breaks shows the ion-specific behaviour; for instance, at $60 \text{ keV}/\mu\text{m}$, protons are fairly dominant in inducing DSB ($\sim 102\text{Gy}^{-1}\text{cell}^{-1}$) compared to helium nuclei ($\sim 87\text{Gy}^{-1}\text{cell}^{-1}$) and carbon ions ($\sim 75\text{Gy}^{-1}\text{cell}^{-1}$). This reduction can be attributed to the decrease in the indirect contribution with increasing LET, which is likely due to the structure of the proton track.

A comparison between the yield results obtained in this work and other simulations and experimental data found in the literature was performed. Our results for proton and α -particles DSB yields follow the same behaviour (DSB yield increasing with LET, for both proton and α -particles) as in other simulations [40, 68]. Such behaviour may be related to the increase of the clustering of energy depositions and chemical species production. Our results for protons are consistent with those reported by Friedland *et al.* [43] where PARTRAC has been used to simulate track structures of protons, α -particles and light ions with low to medium energies. In terms of absolute values, there are discrepancies of less than 2% between these two works for DSB yield due to protons indicating that MCDS algorithm gives reliable results of the damage yields that are comparable to those obtained from computationally expensive but more detailed track structure simulation models. This is as expected since the MCDS simulations implicitly account for both direct and indirect DNA damage mechanisms. For clarity of data points in the effective plot, we do not show the results from these studies. A comparison with the experimental data, however, shows large discrepancies at

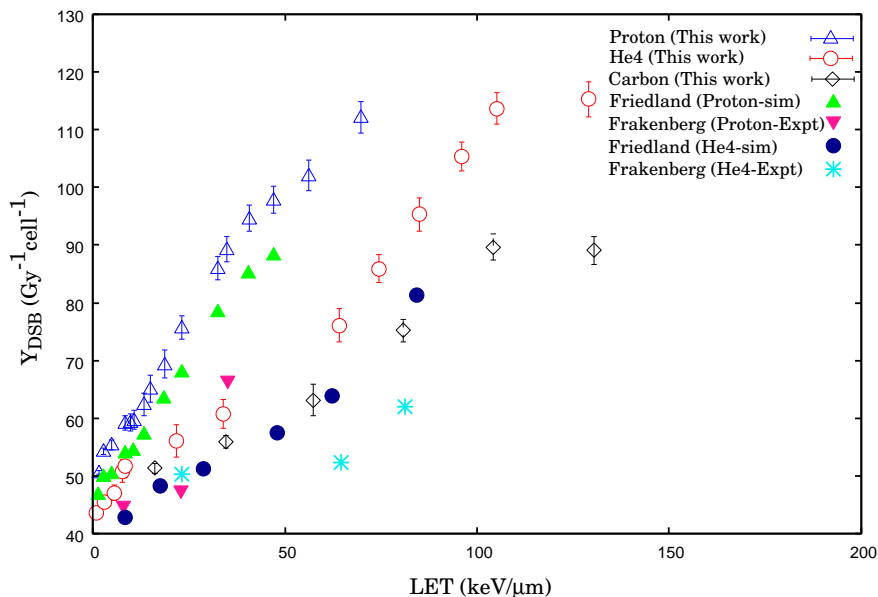


FIG. 1: Yields of radiation-induced DSB with protons (open triangles), He4 (open circles) and carbon ions (open diamonds) as a function of LET. For comparison, we also show the simulation results obtained by Friedland *et al.* [43] using PARTRAC and experimental results of Frakenberg *et al.* [28]

both low and medium LET. This might largely be, among other factors, due to the dependence of experiments on the ability to determine small DNA fragments, similar to the influence of physical and biological models implemented in Monte Carlo algorithms on the simulations.

With the values for DSB yield established for specific hadron species, we obtain the data for α and β parameters of the model and show their dependence on LET in Fig. 2. The surface plots (panels a-d) of linear-quadratic parameters with protons and helium ions in Fig. 2 show different trends with increasing LET and dose. It can be seen that the linear-parameter, α , becomes progressively steeper as the particle LET increases. At a given LET, the alpha parameter for protons (Fig. 2e) is higher than that for the helium and carbon ions. This could be due to increases in proton relative effectiveness for DSB induction in the LET range 5-70 keV/ μ m caused by a difference in the track structures of the ion beams at the same LET through differences in the effective charge and the velocity of the ion. With helium and carbon ions, the linear parameter seemed to increase to a maximum before starting to fall at high LETs. The position of the maximum alpha shifts to higher LET values for carbon ions. The modelled alpha values show a good agreement with the LEM-based results [91], particularly up to approximately 12 keV/ μ m using protons. Beyond this value, the LEM exhibits an enhancement in the linear parameter. Nonetheless, while our parameters α results show a slow increase, compared to LEM model, both show a similar trend as expected. As a result, our α results with proton irradiation are more reliable for low LET values than for high ones. No relevant differences for dose per step and aerobic and hypoxic conditions are apparent up to 8 keV/ μ m. The α values for helium and carbon-ions show a similar trend with nearly the same values at similar LETs under both aerobic and hypoxic conditions.

For medium and high LET values, our simulation results show an almost vanishing β parameter for all radiation types used in this study (Fig. 2f). For helium and carbon-ions, we observe the general trend, an increase at low LET values followed by a decrease at higher LETs, showing that the trends are qualitatively similar across cells of different radiosensitivities. Similar to the α maximum, the fall-off for β is shifted to higher LET for carbon-ion. Again, in terms of the absolute values, the variation trend of our estimated with those of LEM model is significant at low LET values under both aerobic and hypoxic conditions. This may be due to an improved description of the quadratic parameter within the LEM framework [16] as well as in this study (Eq.3), where the variations of dose affect β more than α , especially at high LET values.

Since the α/β is mainly attributed to the number of primary particles that cause DSBs per dose for charged particles at higher LET values, the cell sensitivity has less effect of cell killing for charged particle species. Fig. 3a shows the ratio (on the logarithmic scale) for cells irradiated by various hadrons at different LETs. The initial slope of the ratio increase steeply with LET. This increase is due to an increase in α value (primarily due to the clustered DNA damage effect) with LET as well as the decrease in the interaction of DSBs (contribution to β term of the mechanistic model) induced by different primary particles. This interaction becomes vanishingly small at intermediate LET values. The

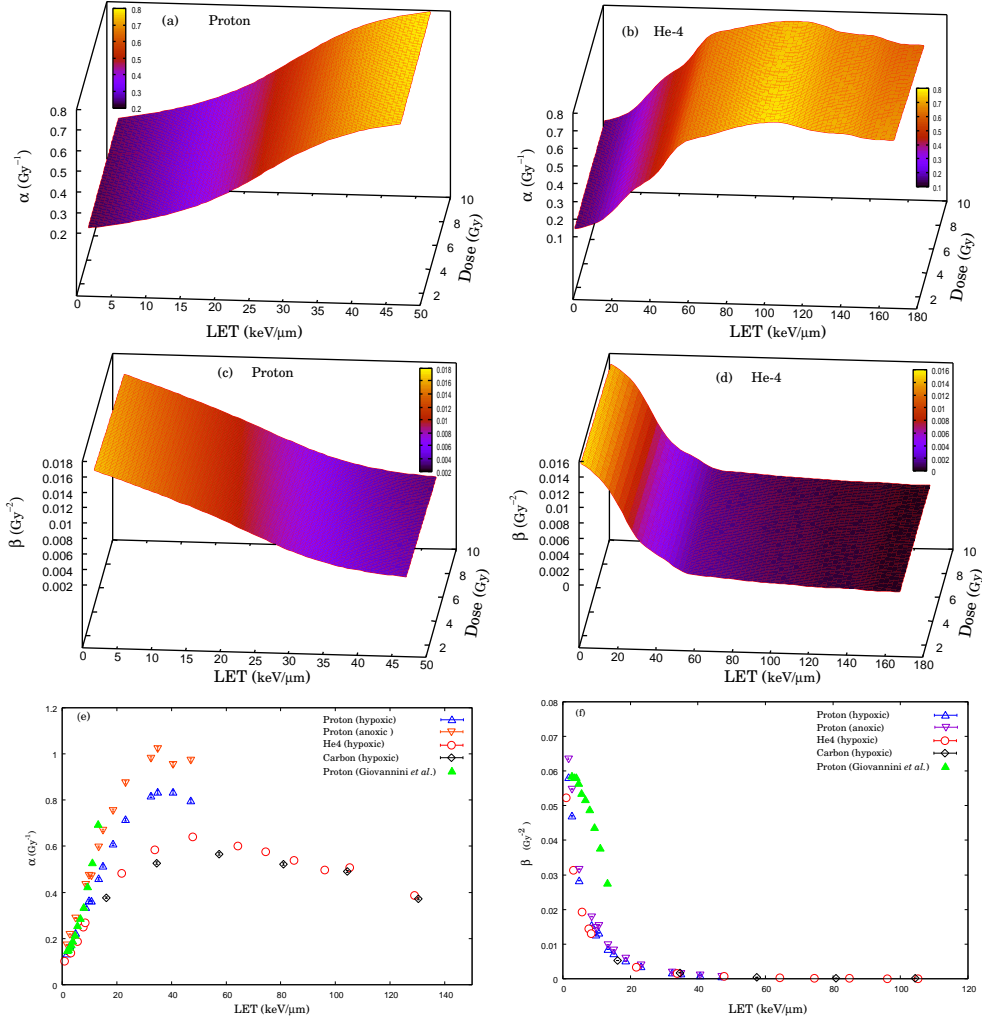


FIG. 2: Linear-quadratic parameters of the model for exposed to protons (panels a and c) and He4 ions (panels b and d) for a range of LET values. Comparison with the results obtained using LEM model [91] is shown in panels (e) and (f).

ratio seems to reach a plateau for high LET values with helium- and carbon ions. This is more likely due to the saturation in the clustered DNA damage and the effect of overkill on cell death.

The question of whether the model parameter are interdependent is an important indicator that needs to be explored. To explore the correlation between the model parameters, we plot the quadratic parameter against linear parameter for different radiation types at different LET-dose combination in Fig. 3b. Whereas, a plateau with no visible interdependence, between the parameter with carbon-ions is observed, the plot suggests a clear negative correlation between the parameters with protons and helium-ions.

For protons and helium, the signal is noisy at earlier α values, and hence we fit a linear regression to the data in the interval $0.3 \leq \alpha \leq 1.0$. The best fit curve to the data gives a negative slope of (-0.0125 ± 0.0013) and has $\chi^2/N_{df} = 0.82$. The fit to the data using helium-ions gives a smaller slope of (-0.0060 ± 0.0014) . The statistical uncertainties on our measurements are typically on the few percent levels. In both the cases, a p -value test, at 5% significance level, was performed on the correlation coefficient between the model parameters with $r_p = -0.8679$ ($p = 0.000057$) and $r_{He} = -0.9162$ ($p = 0.000002$), respectively. These values suggest a correlation between the linear and quadratic parameters for proton and helium-ion irradiation. We will keep a close eye on the trend of the survival curves to see if such an interdependence influences the steepness in the exponential fall of the curves.

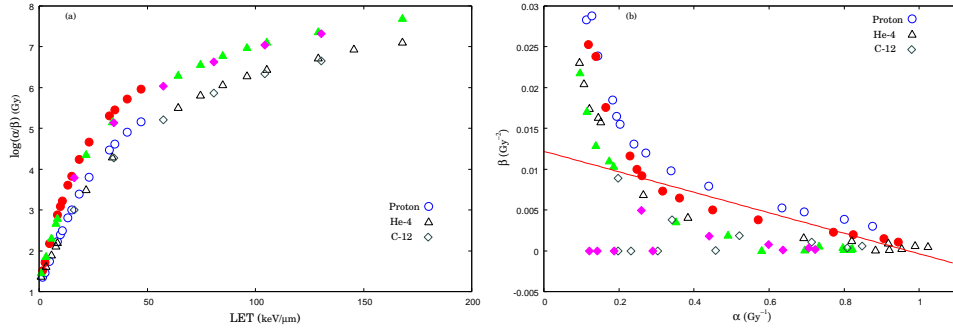


FIG. 3: (a) α/β (in logarithmic scale) as a function of LET. (b) Correlation between LQ parameters of the cancer cells. The open symbols represent the data using protons (open circles), helium-ions (open triangles) and carbon-ions (open diamonds) at 3 Gy dose. The corresponding solid symbols represent the data at 5 Gy. The straight line represents the linear fit to the data using proton irradiation (solid circles).

B. LET-dependent RBE

Whereas a large amount of data from different experimental protocols and biological models are available [39], the adoption of a simple and unique RBE-LET relationship in effective treatment planning is surrounded by a number of uncertainties. Few studies have supported a reasonable approximation of fixed RBE to describe the increased effectiveness of light ions [17, 91–93], the concerns for a better understanding of RBE-LET relationship for significant clinical relationship have been raised. To further explore the impact of LET on radio-sensitivity, we analyse and display in Fig. 4, the RBE corresponding to the initial slope for different particle types, with x-rays as reference radiation ($\alpha_{\text{ref}} = 0.616 \text{Gy}^{-1}$, $\beta_{\text{ref}} = 0.062 \text{Gy}^{-2}$). It is obvious from the effective plots (a-c) that the maximum in RBE depends on the particle species, where heavier particles have the maximum at higher LET values and that the lighter ions provide higher RBE values for a fixed LET. It can be seen from Fig. 4c that RBE decreases with increasing dose. Comparison with other numerical estimates and experimental results shows a good agreement, especially for protons. However, we notice a deviation of our results at high LET value for helium ions, but the overall trend agrees well with those of the observed results for different particle species at different LET.

To explore how RBE compares in the limit of full survival level and 10% survival dose, we collect and display RBE values obtained from the 10% survival when cells are irradiated by different particle species with different LET in Fig. 4d. We notice that the RBE-LET spectra are different for different particle types; RBE with protons increases with LET, peaks at around 45 keV/ μm and then decreases with LET, whereas, for helium-ions, the RBE increases slowly in the medium LET region with a rather broad peak in the near-high LET region. The RBE values show a good agreement with the measured values at small LET for protons but considerable scattered of the experimental values around our numerical estimates with small and medium LET values for helium-ions. The RBE for 10% survival level plots with protons and helium-ions nearly level up in the high-LET region and approach approximately to 1.

As far as the role of sensitizers, such as oxygen, on the radioresistance of the cells is concerned, we extract α and β from the slopes of the survival curve at 10% survival level to calculate OER values using Eq. (5). We notice that a decrease in the OER values for helium and carbon-ions starts at around 50 keV/mm, passing below 2 at around 100 keV/mm, and then reaches approximately 1 (significantly lower for helium-ions) in the very high-LET region. The OER was significantly lower for helium ions than the others. The presence or absence of oxygen mainly affects the initial radiation-induced DSB yield and not the rate of DSB rejoining. However, due to the dominant contribution of direct effect in the high LET region and available oxygen-independent pathway, the dependence on oxygen for cell kill becomes less important.

We conclude this section by exploring the dependence of RBE on cellular repair factor and the radiation type. Note that for smaller values of β/α the RBE increases linearly with an initial slope of (2.11 ± 0.7) Gy and decreases sharply for larger values of β/α with a slope (-4.11 ± 0.7) . The considerable scatter of the data points for various particle types indicate particle specific behaviour of the initial slope of RBE.

The average RBE of protons seems to exceed that of helium- and carbon-ions at smaller β/α value for a given LET by a factor of nearly two. Also, similar to the trend of a shift in maxima of RBE-LET relationship towards higher particle LET for helium and carbon-ions (Fig. 4d), the RBE maxima shifts towards higher values of the ratio α/β . A linear fit of the form $RBE_{3\text{Gy}} = a + b \cdot (\beta/\alpha)$ gives slopes of (-1.59 ± 0.16) and (-1.69 ± 0.20) with $\chi^2/N_{df} = 0.74$ and 0.69 for protons and helium-ions, respectively. This implies that the cells with higher repair factor ratio provide large RBEs for medium and larger doses compared with cells with a smaller α/β ratio. Therefore, tumours with high

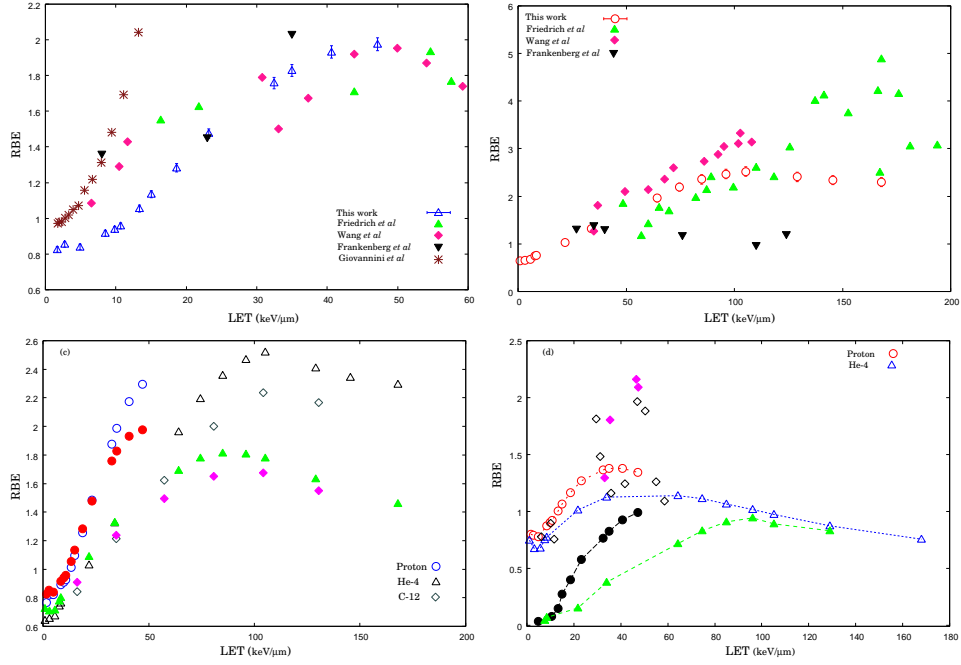


FIG. 4: LET-dependent simulated values of RBE of protons (panel a), helium-ion (panel b). Also, are shown the RBE values obtained from earlier studies for comparison ([28, 39, 40]). Panel (c) shows the RBE values at different doses (open symbols - 3 Gy and filled symbols - 5 Gy). Panel (d) shows RBE values of ionizing radiations at 10% survival level in comparison with values obtained in full survival level.

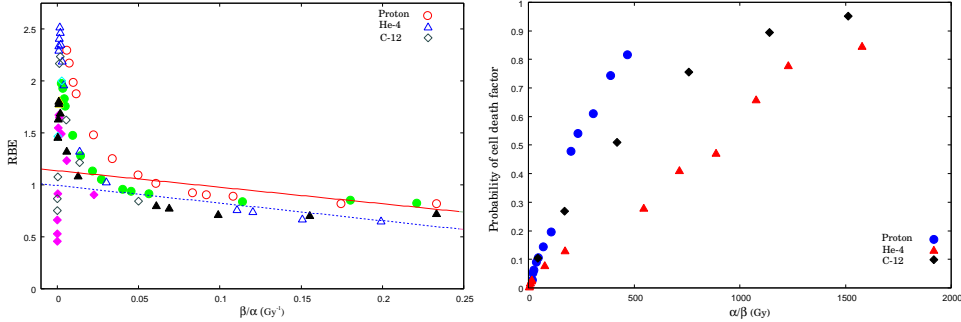


FIG. 5: (Left panel) Dependence of RBE values of ionizing radiations on inverse ratio at 5 Gy dose. The lines are linear fits to the data using protons (open circles) and He-4 ions (open triangles). The corresponding solid symbols represent the data at 10 Gy dose. (Right panel) Probability of cell death factor with changing dose as a function of cellular repair factor using protons, helium and carbon ions.

repair indicators surrounded by healthy tissue with smaller repair indicators are suited for hypofractionated regimens than from normal fraction schemes and vice versa. This clearly indicates that both LET and α/β ratio need to be taken as RBE predictors for any hadrontherapy treatment plan.

Finally, to explore the possibilities in adjusting the radiosensitivity of cells in the model, we plot, in Fig. 5 (right panel), the probability of death cell factor as a function of cellular repair factor α/β . We notice that, compared to heavy ions, the probability of cell death factor increases steeply with proton, with differences attributed to α/β ratio, cellular kinetics and to the way the energy from radiation exposure is deposited.

C. Cell survival curves

Using pulses of dose for cancer cells, we observed that the cell colony grew rapidly at low LET ($< 5 \text{ keV}/\mu\text{m}$) for dose rate $< 20 \text{ mGy/step}$ for all the three radiation types. This is as expected since, under the input conditions, the probability distributions of cell splitting and cell multiplication dominate and dose pluses are insufficient for killing the cancer cells. Also, the adaptive response at low LET-dose proved effectively insufficient to make a contribution to the increase in the frequency of mutations. Whereas the medium and strong adaptive response input signals showed a significant change in mutation frequency, the cell colony continued to grow for low LET-dose values. Proposed dose and LET-dependent cell survival responses are simulated by choosing the minimum LET-dose combination for which the cell survival curves converge after a certain number of time-steps.

We noticed a clear split of the iteration dose-LET spectra among protons, helium-and carbon-ions. At LET $\geq 8.5 \text{ keV}/\mu\text{m}$ and 20 mGy/step dose rate, protons are more effective in cell killing than helium- and carbon ions. Statistically, all the cancer cells are killed after the 80th time step with proton irradiation compared to approximately 65% kill rate by helium-ions. With the pulse of 12 mGy/step at $15 \text{ keV}/\mu\text{m}$, we observed that both protons and carbon-ions have similar cell killing effects, however, there was a noticeable change of mutation frequency.

A relation between representative cell survival and dose-LET was extracted after evaluating dose-LET nomenclature with light and heavy ions. The surface plots of the representative survival curves are not displayed here. It is observed that as the average LET increases, the curves become more steeper and the survival curves with protons converge faster than those from helium ions at low-LET. For most cell types, survival curves start with a moderate slope, and with increasing dose, the slope correspondingly increases. At low doses, survival curves start with a steep slope which decreases at a moderate dose and flattens out with increasing dose. Therefore, the efficiency per dose increment decreases as well. This can be understood in terms of the reparability of radiation induced damages. At low doses, only a few damages are induced with a large spatial separation, and a considerable fraction of these damages can be repaired correctly. In contrast, at high doses, the density of damages increases, leading to an interaction of damages and thus a reduced fraction of repairable damages. The term "interaction" has to be understood here in the most general sense. On the one hand, it can happen, e.g., that actually two individual damages are combined to form a more complex type of damage. On the other hand, two damages produced in close vicinity can lead to conflicting or competing repair processes, also reducing the fraction of repairable damage.

Fig. 6 (a-c panels) collects and displays the survival curves obtained from the simulation outcomes of cells irradiated with protons, helium-ion and carbon-ions and compared to the experimental data selected from [95]. For the low LET, protons seem to be more effective in cell kill than helium-ions. Statistically, only 15% of the cancer cells survive after 20th-time step compared to more than 50% surviving cells with helium-ions at the same LET value. We also notice that surviving curves with helium-ion show a plateau(not shown here) at high doses. This might be due to the shielding of a fraction of cells as a result of the range of helium-ion at these energies not exceeding the width of the cell, thus causing a plateau even at relatively modest surviving fraction levels. Whereas we have not been able to simulate with light and heavy ions that are exactly matched for LET, nevertheless, we notice that at moderate LET, protons and carbon ions are more effective in cell kill than doubly-charged particles of similar LET. It is evident from RBE-LET relationship that the data for ${}^4\text{He}$ indicate a maximum RBE at around 90 - 100 $\text{keV}/\mu\text{m}$ and flattens out at higher LET values, this would explain why helium-ions are less effective than protons with the same LET for cell survival. The increased lethality of protons compared to helium ions in cell survival data are therefore consistent with studies that place importance on the extent to which ionizations are clustered at the nano-scale.

In Fig. 6 (b-d), we extend our investigation to survival curves for cells exposed to helium-and carbon-ions both at medium and high LET. Except for proton data at $56.1 \text{ keV}/\mu\text{m}$ (panel d), where we observed a low mutation frequency and a weak adaptive response signal (not shown here for the sake of clarity), which describes the ability of low-dose radiation to induce cellular changes that alter the level of subsequent radiation-induced damage, the survival curves start with a steep slope, and with increasing dose, the slope decreases. Therefore, the efficiency per dose increment decreases as well. We notice that the dose-response relationship of the surviving curves is generally non-linear. This is because of the quasi-linear/sigmoidal multiple input dose-dependent relationships, internal conditions, dependencies, and cancer cell transformation where simplified biology was described by non-trivial probability distributions and random processes that are close to real situations. Such a behaviour of organism response has previously been observed in many other studies [96, 97]

The shape of the survival curves change from low dose in character to high dose; the curves start showing a non-linear behaviour as the cumulative dose increases. This might be related to the reparability of radiation-induced damages and mutation frequency. At high doses, only a few damages are induced due to shielding, and a considerable fraction of these damages can be repaired correctly. In contrast, at low and medium doses, the density of damages increases, leading to an interaction of damages and thus a reduced fraction of repairable damages. From the above surviving curves it can be seen that at low and medium LET values here, protons show increased effectiveness with increasing LET.

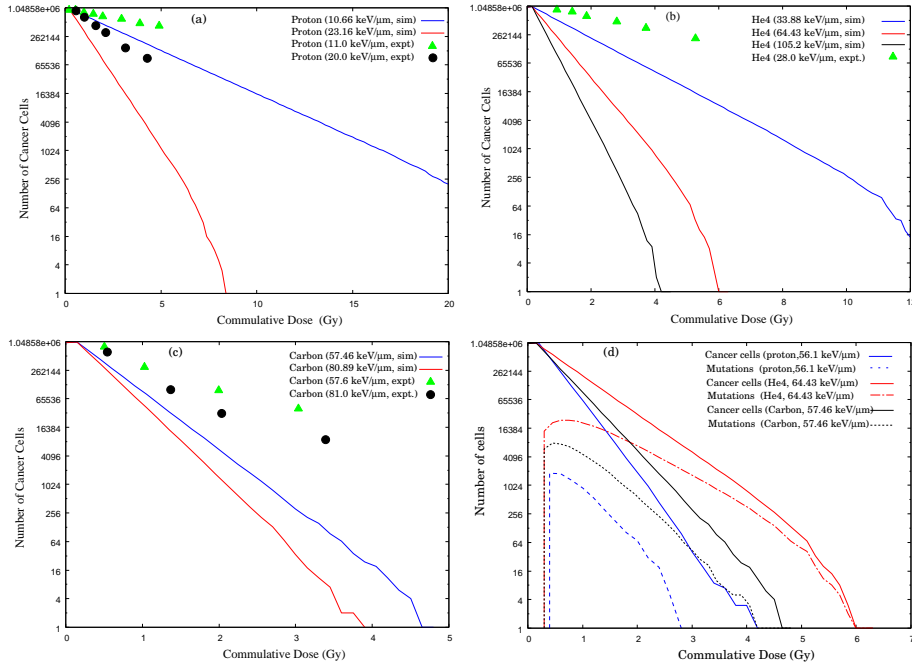


FIG. 6: Survival curves after exposure to protons (panel a), helium ions (panel b), and carbon ions (panel c) compared with the results from the experimental data [95]. Panel (d) shows the fraction of cancer and mutation cells with different particle species.

In light of the discussion above, it is reasonable to expect that despite the discrepancies, our simulated survival curves for low LET protons, helium- and carbon-ions are in good general agreement with the considered experimental data. This serves one of the aims of the model to predict the relationship between radiation-induced DSBs in the cell nucleus and cell survival probability. This supports the hypothesis of the mechanistic model that interaction among DSBs induced by ionizing radiation contribute to the quadratic term of the model, therefore the cell survival curves are in agreement with the measured data for low-LET particle species.

V. SUMMARY AND CONCLUSION

A stochastic Monte Carlo technique was used to simulate a full grown colony of cancer cells using a mechanistic model of cellular survival following radiation induced DSBs. Simulations were performed using light and heavy-ion species over a range of LET values. To make the model more realistic, we incorporated, following the theories of nucleation and growth, individual susceptibilities and probabilities as quasi-linear and sigmoidal input relations described by various probability distributions and random processes that apply for the effects like radiation-induced mutation, cell transformation, and multiplication, hadroadaptive response, cancer cell kill and more. This is a significant improvement of the linear assumption for stochastic cancer effect used frequently. Hypoxia was implemented through random assignment of partial oxygen pressure values to individual cells during tumour irradiation. The uncertainties in the measurements are estimated by binning the numerical data into 10 blocks. The mean and the final errors of the observables obtained using a single-elimination jackknife method with each bin regarded as an independent data point.

The yield of radiation induced DSB and DSB yield per cell per primary particle was calculated using a fast Monte Carlo damage simulation algorithm. At high LET, the estimated DSB yields showed ion-specific characteristics. Above 12 keV/μm, proton showing most effectiveness in inducing DSB than heavier ions at the same LET. Our DSB yield results at low LET showed consistency with those obtained using LEM model-based data with proton irradiation.

The LET-dependent DSB yield for different particle species was used to calculate the α , β and α/β ratio, using the improved descriptions of their definitions in the model. The simulation results predict a gradual increase in α , β , and the ratio α/β as a function of LET which is consistent qualitatively with the cell-inactivation target theory. The ratio showed a quick increase with LET, indicating a cluster DNA damage effect and a decrease in interaction of DSBs induced by different primary particles. At high LET, the contribution of quadratic parameter β was found

to be vanishingly small. It was also observed that the cells with a higher α/β ratio provide large RBEs for low and medium doses compared with cells with smaller α/β ratios. This implies that the tumours with high repair indicators surrounded by healthy tissue with smaller repair indicators are suited for hypofractionated regimens than from normal fraction schemes and vice versa. At the medium doses, the RBE values seem more or less insensitive to the ratio. This clearly indicates that both LET and α/β ratio need to be taken as RBE predictors for any hadrontherapy treatment plan. The predicted estimates of RBE at the initial slopes and at 10% survival that are in good agreement with the experimental data. Since the values of α and β change with LET, the dependence of RBE on particle species and the cellular repair capacity was modelled by LET-dependent RBE model. These findings suggest that it is worth considering at least main RBE dependencies in treatment planning, and being particularly cautious for tissues with a low α/β ratio. This is in contrast with some earlier studies which support the conclusions that RBE dependence on cell type and particle species is small enough to be safely neglected.

Finally, from the surviving curves, it becomes clear that although most of the dose-LET and given observable relationships are linear, the dose-response outcome is more complex than the one predicted by the oversimplified LQ model. Another interesting feature was the rapid increase in the probability of cell death relative to probability of its multiplication and number of mutations per cancer cell with increasing dose-LET values. Despite this, the model still reproduces the behaviour of cell lines well across a range of conditions without cell-line specific fitting parameters. Thus while exact quantification of, for example, α/β ratios may prove challenging for a specific experimental condition, the model still has the potential to make useful predictions about overall sensitivity.

While the current approach is sufficient to demonstrate the viability of the model, explicitly incorporating models of the underlying genetic pathways driving these effects will enable more granular models of the impact of tumour genetics. The cell survival probability does not reflect and explicate damage caused by DNA single-strand breaks which could be many times more than the number of DSBs, as well as SSB damage conversion into DSB damage resulting in the stop of cell proliferation. This might demand for an improved description of the biological and physical process in cell survival probability defined LQ-theory. We intend to improve the model and the algorithm to incorporate cancer-specific factors, such as DNS single-strand break and cell proliferation before reproductive death in the conventional LQ-theory as well as complex biology of the cancer cells and more complex tissue reactions.

VI. ACKNOWLEDGMENTS

We wish to thank Krzysztof Fornalski for a number of valuable suggestions, which provided the impetus for much of this work. The computations for DNA damage were done using a modified version of publicly available MCDS code (see <http://faculty.washington.edu/trawets/mcnds>). We are also grateful for access to KCST computing facility.

References

-
- [1] M. Carante and F. Ballarini, *Modelling cell death for cancer hadrontherapy*, AIMS Biophysics, **4**, 465 (2017)
 - [2] F. Tommasino and M. Durante, *Proton Radiobiology*, Cancers, **7**, 353 (2015)
 - [3] M. Regler, M. Benedikt, and K. Poljanc, Proc. Regler Medical AF (2009)
 - [4] P. Kundrat, *Detailed analysis of the cell-inactivation mechanism by accelerated protons and light ions*, Phys. Med. Biol. **51**, 1185 (2006)
 - [5] R. Mayer, *Stereotactic radiotherapy for primary lung cancer and pulmonary metastases: A noninvasive treatment approach in medically inoperable patients*, Radiother. Oncol. **73** (Suppl. 2) S24 (2004)
 - [6] M. Krengli and R. Orecchia, *Medical aspects of the National Centre for Oncological Hadrontherapy*, Radiother. Oncol. **73**, (Suppl. 2), S21 (2004)
 - [7] A. Brahme, R. Lewensohn, U. Ringborg, U. Amaldi, F. Gerardi and S. Rossi, *Design of a centre for biologically optimised light ion therapy in Stockholm*, Nucl. Instrum. Methods **B 184**, 569 (2001)
 - [8] N. Tilly, A. Brahme, J. Carlsson and B. Glimelius, *Comparison of cell survival models for mixed LET radiation*, Int. J. Radiat. Biol. **75**, 233 (1999)
 - [9] F. Tommasino, E. Scifoni and M. Durante, *New ions for therapy*, Int. J. Part. Ther. **2**, 428 (2015)
 - [10] U. Linz, *Physical and Biological Rationale for Using Ions in Therapy*, Ion Beam Therapy, Springer Berlin Heidelberg, 45, (2012)
 - [11] M. Durante and J. Loeffler, *Physical and Biological Rationale for Using Ions in Therapy*, Nat Rev. Clin. Oncol. **7**, 37 (2010)
 - [12] U. Amaldi and G. Kraft, *Radiotherapy with beams of carbon ions*, Rep. Prog. Phys. **68**, 1861 (2005)

- [13] H. Paganetti and P. van Luijk, *Biological considerations when comparing proton therapy with photon therapy*, Semin. Radiat. Oncol. **23**, 77 (2013)
- [14] S. Girdhani, R. Sachs and L. Hlatky, *Biological effects of proton radiation: what we know and don't know*, Radiat. Res. **179**, 257 (2013)
- [15] T. Friedrich, U. Scholz, T. Elsasser, M. Durante and M. Scholz, *Systematic analysis of RBE and related quantities using a database of cell survival experiments with ion beam irradiation*, J. Radiat. Res. **54**, 494 (2012)
- [16] T. Friedrich, U. Scholz, T. Elsasser, M. Durante and M. Scholz, *Calculation of the biological effects of ion beams based on the microscopic spatial damage distribution pattern*, Int. J. Radiat. Biol. **88**, 103 (2012)
- [17] H. Paganetti *et al.*, *Relative biological effectiveness (RBE) values for proton beam therapy*, Int. J. Radiat. Oncol. Biol. Phys. **53**, 407 (2002)
- [18] J. Ward, W. Blakely and E. Joner, *Mammalian cells are not killed by DNA single-strand breaks caused by hydroxyl radicals from hydrogen peroxide*, Radiat. Res. **103**, 383 (1985)
- [19] J. Ward, *DNA damage produced by ionizing radiation in mammalian cells: identities, mechanisms of formation, and reparability*, Prog. Nucleic Acid Res. Mol. Biol. **35**, 95 (1988)
- [20] J. Ward, *Radiation mutagenesis: the initial DNA lesions responsible*, Radiat. Res. **142**, 362 (1995)
- [21] M. Belli M, *et al.*, *DNA fragmentation in V79 cells irradiated with light ions as measured by pulsed-field gel electrophoresis. I. Experimental results*, Int. J. Radiat. Biol. **78**, 475 (2002)
- [22] C. Leloup, *et al.*, *Evaluation of lesion clustering in irradiated plasmid DNA*, Int. J. Radiat. Biol. **81**, 41 (2005)
- [23] M. Hada and B. Sutherland, *Spectrum of complex DNA damages depends on the incident radiation*, Radiat. Res. **165**, 223 (2006)
- [24] V. Calugaru, C. Nauraye, G. Noel, N. Giocanti, V. Favaudon, and F. Megnin-Chanet, *Radiobiological characterization of two therapeutic proton beams with different initial energy spectra used at the Institut Curie Proton Therapy Center in Orsay*, Int. J. Radiat. Oncol. Biol. Phys. **81**, 1136 (2011)
- [25] K. Prise *et al.*, *A review of dsb induction data for varying quality radiations*, Int. J. Radiat. Biol. **74**, 173 (1998)
- [26] K. Prise, M. Pinto, H. Newman and B. Michael, *A review of studies of ionizing radiation-induced double-strand break clustering*, Radiat. Res. **156**, 572 (2001)
- [27] M. Belli *et al.*, *DNA double-strand breaks induced by low energy protons in V79 cells*, Int. J. Radiat. Biol. **65**, 529 (1994)
- [28] H. Frankenberg *et al.*, *Induction of DNA Double-Strand Breaks by ^1H and ^4He Ions in primary human skin fibroblasts in the LET range of 8 to 124 keV/ μm* , Radiat. Res. **151**, 540 (1999)
- [29] M. Belli *et al.*, *DNA fragmentation in mammalian cells exposed to various light ions*, Adv. Space Res. **27**, 393 (2001)
- [30] M. Belli *et al.*, *DNA DSB induction and rejoining in V79 cells irradiated with light ions: a constant field gel electrophoresis study*, Int. J. Radiat. Biol. **76**, 1095 (2000)
- [31] M. Pinto, K. M. Prise and B. D. Michael, *Quantification of radiation induced DNA double-strand breaks in human fibroblasts by PFGE: testing the applicability of random breakage models*, Int. J. Radiat. Biol. **78**, 375 (2002)
- [32] M. Carante *et al.*, *Modeling radiation-induced cell death: role of different levels of DNA damage clustering*, Radiat. Environ. Biophys. **54**, 305 (2015)
- [33] I. El Naqa, P. Pater, P. and J. Seuntjens, *Monte Carlo role in radiobiological modelling of radiotherapy outcomes*, Phys. Med. Biol. **57**, R75 (2012)
- [34] C. Wang, *The progress of radiobiological models in modern radiotherapy with emphasis on the uncertainty issue*, Mutat. Res. **704**, 175 (2010)
- [35] R. Dale, B. Jones and A. Carabe-Fernandez, *Why more needs to be known about RBE effects in modern radiotherapy*, Appl. Radiat. Isot. **67**, 387 (2009)
- [36] M. Kramer *et al.*, *Treatment planning for heavy-ion radiotherapy: physical beam model and dose optimization*, Phys. Med. Biol. **45**, 3299 (2000)
- [37] M. Kramer *et al.*, *Treatment planning for heavy-ion radiotherapy: calculation and optimization of biologically effective dose*, Phys. Med. Biol. **45**, 3319 (2000)
- [38] K. Kagawa *et al.*, *Preclinical biological assessment of proton and carbon ion beams at Hyogo Ion Beam Medical Center*, Int. J. Oncol. Biol. Phys. **54**, 928 (2002)
- [39] T. Friedrich *et al.*, *Systematic analysis of RBE and related quantities using a database of cell survival experiments with ion beam irradiation*, J. Radiat. Res. **10**, 1093 (2012)
- [40] W. Wang, C. Li, R. Qiu, Y. Chen, Z. Wu, H. Zhang and J. Li, *Modelling of cellular survival following radiation-induced DNA double-strand breaks*, Sci. Rep. **8**, 16202 (2018)
- [41] R. Abolfath *et al.*, *A model for relative biological effectiveness of therapeutic proton beams based on a global fit of cell survival data*, Sci. Rep. **7**, 8340 (2017)
- [42] S. McMahon, A. McNamara, J. Schuemann, H. Paganetti and K. Prise, *A general mechanistic model enables predictions of the biological effectiveness of different qualities of radiation*, Sci. Rep. **7**, 10790 (2017)
- [43] W. Friedland, *et al.*, *Comprehensive track-structure based evaluation of DNA damage by light ions from radiotherapy-relevant energies down to stopping*, Sci. Rep. **7**, 45161 (2017)
- [44] S. McMahon, J. Schuemann, H. Paganetti and K. Prise, *Mechanistic Modelling of DNA Repair and Cellular Survival Following Radiation-Induced DNA Damage*, Sci. Rep. **6**, 33290 (2016)
- [45] R. Hawkins, *A microdosimetric-kinetic theory of the dependence of the RBE for cell death on LET*, Med. Phys. **25**, 1157 (1998)
- [46] R. Hawkins, *A microdosimetric-kinetic model for the effect of non-Poisson distribution of lethal lesions on the variation of RBE with LET*, Radiat. Res. **160**, 61 (2003)

- [47] M. Scholz and G. Kraft, *track structure and calculation of biological effects of heavy charged particles*, Adv. Space Res. **18**, 5 (1996)
- [48] M. Scholz, *Calculation of RBE for normal tissue complications based on charged particle track structure*, Bull Cancer Radiother. **83** (Suppl.), 50s (1996)
- [49] M. Scholz, M. A. Kellerer, W. Kraft-Weyrather and G. Kraft, *Computation of cell survival in heavy ion beams for therapy. The model and its approximation*, Radiat. Environ. Biophys. **36**, 59 (1997)
- [50] C. Karge and P. Peschke, *RBE and related modeling in carbon-ion therapy*, Phys. Med. Biol. **63**, 01TR02 (35pp) (2018)
- [51] S. Sawant, G. Randers-Pehrson, N. Metting and J. Hall, *Adaptive Response and the Bystander Effect Induced by Radiation in C3H 10T Cells in Culture*, Radiat Res **156**, 177 (2001)
- [52] L. Feinendegen, V. Bond, C. Sondhaus and H. Muehlensiepen, *Cellular signal adaptation with damage control at low doses versus the predominance of DNA damage at high doses*, Mutat. Res **358** 199 (1996)
- [53] L. Feinendegen, V. Bond, C. Sondhaus and K. Altman, *Cellular signal adaptation with damage control at low doses versus the predominance of DNA damage at high doses*, Acad. Sci. Paris, Life Sci. **322** 245 (1999)
- [54] E. Azzam, S. de Toledo, G. Raaphorst and R. Mitchel, *Responses to Low Doses of Ionizing Radiation in Biological System*, Radiat. Res. **146**, 369 (1996)
- [55] R. Mitchel *et al.*, *The Adaptive Response Modifies Latency for Radiation-Induced Myeloid Leukemia in CBA/H Mice*, Radiat. Res. **152**, 273 (1999)
- [56] M. William, *Low-dose radiation: Thresholds, bystander effects, and adaptive responses*, PNAS **100**, 4973 (2003)
- [57] L. de Saint-Georges, *Low-dose ionizing radiation exposure: understanding the risk for cellular transformation*, J. Biol. Regul. Homeost. Agents **18**, 96 (2004)
- [58] B. Shankar, R. Pandey and K. Sainis, *Radiation-induced bystander effects and adaptive response in murine lymphocytes*, Int. J. Radiat. Biol. **82**, 537 (2006)
- [59] B. Leonard, *Repair of multiple break chromosomal damageits impact on the use of the linear-quadratic model for low dose and dose rates. In: The Effects of Low and Very Low Doses of Ionizing Radiation on Human Health*, University of Versailles, Elsevier Science B.V. Amsterdam, The Netherlands, 449462
- [60] B. Leonard, 2005, *Adaptive response by single cell radiation hitsImplications for nuclear workers*, Radiation Protection Dosimetry, **116**, 387 (2005)
- [61] B. Leonard, *Adaptive response and human risks: Part IA microdosimetry dose dependent model*, Int. J. Radiat. Bio. **83**, 115 (2007)
- [62] B. Leonard, *Adaptive response: Part IIModeling for dose rate and time influences*, Int. J. Radiat. Bio. **83**, 395 (2007)
- [63] B. Leonard, *Thresholds and transitions for activation of cellular radioprotective mechanismscorrelations between HRS/IRR and the inverse dose-rate effec*, Int. J. Radiat. Bio. **83**, 479 (2007)
- [64] M. Jioner and A. van der Kogel, Basic Clinical Radiobiology, CRC Press, Boca Raton, Fla, USA, 2009
- [65] P. Crooke and F. Parl, *A Mathematical Model for DNA Damage and Repair*, J. Nucl. Acids, **2010**, 1, (2010)
- [66] R. Taleei, M. Weinfeld and H. Nikjoo, *Single strand annealing mathematical model for double strand break repair*, Radiat. Prot. Dosimetry, **143**, 191 (2011)
- [67] X. Deng *et al.*, *Human replication protein A-Rad52-single-stranded DNA complex: stoichiometry and evidence for strand transfer regulation by phosphorylation*, Biochem. **48**, 6633 (2009)
- [68] S. Meylan *et al.*, *Simulation of early DNA damage after the irradiation of a fibroblast cell nucleus using Geant4-DNA*, Sci. Rep. **7**, 11923 (2017)
- [69] L. Garcia, J. Leblanc, D. Wilkins and G. Raaphorst, *Fitting the linear-quadratic model to detailed data sets for different dose ranges*, Phys. Med. Biol. **51**, 2813 (2006)
- [70] L. Garcia, D. Wilkins and G. Raaphorst, *α/β ratio, a dose range dependence*, Int. J. Radiat. Oncol. Biol. Phys. **67**, 587 (2007)
- [71] T. Wenzl and J. Wilkens, *Theoretical analysis of the dose dependence of the oxygen enhancement ratio and its relevance for clinical applications*, Radiat. Oncol. **6**, 171 (2011)
- [72] J. Wilkens, *Modelling of the oxygen enhancement ratio for ion beam radiation therapy*, Phys. Med. Biol. **56**, 3251 (2011)
- [73] H. Tsujii *et al.*, *Clinical results of carbon ion radiotherapy at NIRS*, J Radiat. Res **48** (Suppl A), A1 (2008)
- [74] H. Tsujii *et al.*, *Clinical advantages of carbon-ion radiotherapy*, New Journal of Physics **10**, 075009 (2008)
- [75] M. Suzuki *et al.*, *he PCC assay can be used to predict radiosensitivity in biopsy cultures irradiated with different types of radiation*, Oncol Rep. **16**, 1293 (2006)
- [76] V. Semenenko and R. Stewart, *A Fast Monte Carlo Algorithm to Simulate the Spectrum of DNA Damages Formed by Ionizing Radiation*, Radiat. Res. **161**, 451 (2004)
- [77] R. Stewart *et al.*, *Rapid MCNP Simulation of DNA Double Strand Break (DSB) Relative Biological Effectiveness (RBE) for Photons, Neutrons, and Light Ions*, Phys. Med. Biol. **60**, 8249 (2015)
- [78] K. Fornalski, L. Dobrzynski and M. Janiak, *A Stochastic Markov Model of Cellular Response to Radiation*, Dose-Response, **9**, 477 (2011)
- [79] K. Fornalski, *Mechanistic model of the cells irradiation using the stochastic biophysical input*, Int. J. Low. Radiat. **9**, 370 (2014)
- [80] J. Forster *et al.*, *Simulation of head and neck cancer oxygenation and doubling time in a 4D cellular model with angiogenesis*, Sci. Rep., **7**, 11037 (2017)
- [81] E. Lartogau *et al.*, *Why do patients with weight loss have a worse outcome when undergoing chemotherapy for gastrointestinal malignancies*, Eur. J. Cancer, bf 34, 856 (1998)
- [82] K. Maseide and K. Rofstad, *Mathematical modeling of chronical hypoxia in tumors considering potential doubling time and*

- hypoxic cell lifetime*, *Radiother. Oncol.* **54**, 171 (2000)
- [83] L. McElwain and J. Pettet, *BMJ*, **341**, 4684 (1993)
- [84] K. Borkenstein *et al.*, *Modeling and Computer Simulations of Tumor Growth and Tumor Response to Radiotherapy*, *Radiat Res.* **162**, 71 (2004)
- [85] G. Marsaglia and W. Tsang, *The Ziggurat Method for Generating Random Variables*, *Journal of Statistical Software*, **5**, 1, (2000)
- [86] S. Choen *et al.*, *Nucleated polymerization with secondary pathways. I. Time evolution of the principal moments*, *J Chem Phys.* **135**, 065105 (2011)
- [87] C. Harting, P. Peschke and C. Karger, *computer simulation of tumour control probabilities after irradiation for varying intrinsic radio-sensitivity using a single cell based mode*, *Acta Oncol.* **49**, 1354 (2010)
- [88] E. Hall, 5th ed. Philadelphia: Lippincott Williams & Wilkins (2000).
- [89] H. Nikjoo, P. O'Neill, W. Wilson and D. Goodhead, *Computational Approach for Determining the Spectrum of DNA Damage Induced by Ionizing Radiation*, *Radiat. Res.* **156**, 577 (2001)
- [90] W. Friedland *et al.*, *Simulation of DNA damage after proton irradiation.*, *Radiat. Res.* **159**, 401 (2003)
- [91] G. Giovannini *et al.*, *Variable RBE in proton therapy: comparison of different model predictions and their influence on clinical-like scenarios*, *Radiat. Oncol.* **11**, 68 (2016)
- [92] H. Paganetti *et al.*, *A phenomenological model for the relative biological effectiveness in therapeutic proton beams*, *Phys. Med. Biol.* **59**, R419 (2006)
- [93] C. van Leeuwen *et al.*, *The alfa and beta of tumours: a review of parameters of the linear-quadratic model, derived from clinical radiotherapy studies*, *Radiat. Oncol.* **13**, 96 (2018)
- [94] E. Hoglund *et al.*, *DNA damage induced by radiation of different linear energy transfer: initial fragmentation*, *Int. J. Radiat. Biol.*, **76**, 539 (2000)
- [95] F. Guan *et al.*, *Spatial mapping of the biologic effectiveness of scanned particle beams: towards biologically optimized particle therapy*, *Sci. Rep.* **5**, 9850 (2015)
- [96] N. Zyuzikov, *et al.*, *Lack of nontargeted effects in murine bone marrow after low-dose in vivo X irradiation*, *Radiat. Res.* **175**, 332 (2011)
- [97] T. Henriken and H. Maillie, *Cellular radiation damage and repair*, Chap 12, *Radiation and Health*, Chap 12, pp246, Taylor and Francis (2003)